

Pair Superfluid and Supersolid of Correlated Hard-Core Bosons on a Triangular Lattice

Hong-Chen Jiang

*Kavli Institute for Theoretical Physics, University of California, Santa Barbara, CA 93106, USA and
Center for Quantum Information, IIIS, Tsinghua University, Beijing, 100084, China*

Liang Fu

Department of Physics, Massachusetts Institute of Technology, Cambridge, MA 02139, USA

Cenke Xu

Department of Physics, University of California, Santa Barbara, CA 93106, USA

(Dated: March 2, 2013)

We have systematically studied the hard-core Bose-Hubbard model with correlated hopping on a triangular lattice using density-matrix renormalization group method. A rich ground state phase diagram is determined. In this phase diagram there is a supersolid phase and a pair superfluid phase due to the interplay between the ordinary frustrated boson hopping and an unusual correlated hopping. In particular, we find that the quantum phase transition between the supersolid phase and the pair superfluid phase is continuous.

PACS numbers: 67.80.kb, 67.85.Bc, 67.85.De, 03.75.Lm, 64.60.Bd

I. INTRODUCTION

The Bose-Hubbard model, as the first explicit example of quantum phase transition, has been studied extensively with many techniques. The simplest version of Bose-Hubbard model only involves a Mott insulator phase and a superfluid phase¹, and the quantum phase transition between these two phases can be well-described by a semiclassical Landau-Ginzburg theory. For example, in two dimension, this quantum phase transition is either an ordinary 3d XY transition or a $z = 2$ mean field transition depending on the chemical potential. In the last few years, it was proposed that various extended Bose-Hubbard models can have much richer and more exotic behaviors. For example, a Z_2 topological liquid phase has been discovered in an extended Bose-Hubbard model on the Kagomé lattice²⁻⁵, and in the same model an exotic quantum phase transition between the Z_2 liquid and a conventional superfluid phase was identified⁶. Also, with an extra ring exchange term, it was demonstrated both numerically and analytically that the Bose-Hubbard model can have an exotic fractionalized Bose metal phase⁷⁻⁹.

With a hard core constraint, *i.e.* doubly occupied sites are removed from the Hilbert space, the Bose-Hubbard model is equivalent to a spin-1/2 model. Due to the rapid development of numerical techniques, exotic phases have been identified in many quantum spin-1/2 models as well. For example, based on the density-matrix renormalization group (DMRG) method, a fully gapped topological liquid phase has been discovered in the Kagomé lattice spin-1/2 Heisenberg model^{10,11}, as well as the $J_1 - J_2$ Heisenberg model on the square lattice¹².

In this paper, using the DMRG method, we demonstrate that in one simple extended hard core Bose-

Hubbard model, there are three different interesting phenomena: first of all, there is a supersolid (SS) phase, where there is a coexistence of the off-diagonal long range order of boson creation operator, and a boson density wave order. Secondly, there is a pair superfluid (PSF) phase, where $\langle b_i \rangle = 0$ while $\langle b_i b_{i+\alpha} \rangle \neq 0$. This pair superfluid phase is an analogue of the charge-4e superconductor that was discussed lately^{13,14}. Thirdly, we show that there is a continuous quantum phase transition between the supersolid and the pair superfluid phase.

II. MODEL HAMILTONIAN

We consider a hard-core Bose-Hubbard model with a correlated hopping on a triangular lattice

$$H = t \sum_{\langle ij \rangle} (b_i^\dagger b_j + h.c.) + V \sum_{\langle ij \rangle} n_i n_j - K \sum_{ijk \in \Delta} (n_i b_j^\dagger b_k + h.c.), \quad (1)$$

where b_i^\dagger (b_i) is the boson creation (annihilation) operator and n_i is the boson number operator on site i . In this Hamiltonian t is the ordinary nearest-neighbor (NN) boson hopping amplitude, and V is the NN repulsive interaction. K is a correlated hopping term, and $ijk \in \Delta$ are three sites in a small triangle (shown in Fig.1) of the lattice. We will see that the presence of the K term significantly enriches the phase diagram of this model. In the numerical simulations, for simplicity, we will always set $t = 1$ as the unit of energy, and focus on the case with $V > 0$ and $K > 0$. Notice that here the boson hopping term is frustrated.

We determine the ground-state phase diagram of the model Hamiltonian Eq. (1) by extensive and highly accu-

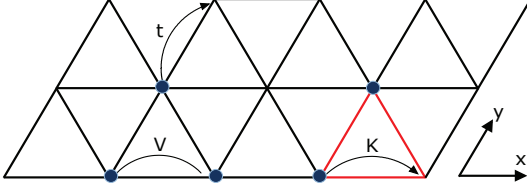


FIG. 1: (Color online) Illustration of the 3-leg ladder geometry with unit vectors $\hat{x} = (1, 0)$ and $\hat{y} = (\frac{1}{2}, \frac{\sqrt{3}}{2})$. The boson hopping strength is t , and the repulsive interaction is V . The correlated hopping term K moves a hard-core boson from one site to another one, depending on the number of boson in the third site in the same small triangle.

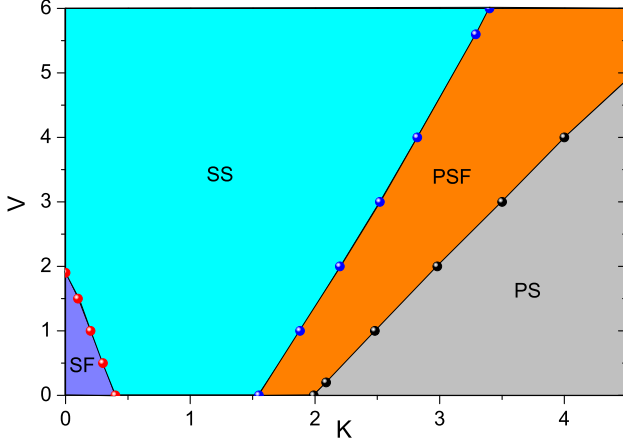


FIG. 2: (Color online) Ground state phase diagram for the correlated hard-core Bose-Hubbard model (Eq. (1)) in a triangular lattice at filling $\rho = 1/6$, as determined by accurate DMRG calculations on cylinders with L_y up to 9. Changing the coupling parameters V and K , four different phases are found, including the superfluid (SF), supersolid (SS), pair superfluid (PSF), and the phase separation (PS).

rate DMRG^{15,16} simulations. In particular, we consider a system with total number of sites $N = L_x \times L_y$, which are spanned by multiples $L_x \hat{x}$ and $L_y \hat{y}$ of the unit vectors $\hat{x} = (1, 0)$ and $\hat{y} = (\frac{1}{2}, \frac{\sqrt{3}}{2})$. For the DMRG calculation, we consider both a cylinder boundary condition (CBC) and a fully periodic boundary condition. Here, CBC means open boundary condition along L_x direction, while periodic boundary condition along L_y direction. This allows us to work on numerous cylinders with much larger system size to reduce the finite-size effect for a more reliable extrapolation to the thermodynamic limit. We keep more than $m = 6000$ states in each DMRG block for most systems, which is found to give excellent convergence with tiny truncation errors that can be fully neglected.

III. PHASE DIAGRAM

The main result of this paper is illustrated in the phase diagram of the model (Eq.(1)) at filling $\rho = \frac{1}{6}$, as shown in Fig.2, obtained by extensive DMRG studies on numerous cylinders with $L_y = 3 - 9$. The nature of the ground state of the model Hamiltonian Eq.(1) at half filling has already been studied previously without considering the correlated hopping term K , where a super-solid phase was found to be stable over a wide range of interaction strength¹⁷⁻¹⁹. In the SS phase there is a long range order of both the boson creation operator and the boson density wave. Further study²⁰ shows that this SS phase will also survive at low boson density, such as $\rho = \frac{1}{6}$, when the repulsive interaction is strong enough. For weak interaction, this SS phase will give way to the simple atomic superfluid phase.

In our current paper, we demonstrate that the unfrustrated correlated hopping term will compete with the repulsive interaction and lead to an interesting phase diagram. In particular, with intermediate strength of K , the SS phase is driven into a uniform pair superfluid phase where $\langle b_i \rangle = 0$, while $\langle b_i b_{i+\alpha} \rangle \neq 0$.

To analyze the ground state properties of the system, we calculate both the density structure factor

$$S(\mathbf{k}) = \frac{1}{N} \sum_{ij} e^{i\mathbf{k} \cdot (\mathbf{r}_i - \mathbf{r}_j)} \langle (n_i - \rho)(n_j - \rho) \rangle, \quad (2)$$

and the momentum distribution function

$$M_b(\mathbf{k}) = \frac{1}{N} \sum_{ij} e^{i\mathbf{k} \cdot (\mathbf{r}_i - \mathbf{r}_j)} \langle b_i^\dagger b_j \rangle, \quad (3)$$

where ρ is the filling factor of the system. We also calculate the pair superfluid structure factor

$$M_p^\alpha(\mathbf{k}) = \frac{1}{N} \sum_{ij} e^{i\mathbf{k} \cdot (\mathbf{r}_i - \mathbf{r}_j)} \langle \Delta_i^+ \Delta_j^\alpha \rangle, \quad (4)$$

to characterize the pair superfluid phase. Here $\Delta_i^\alpha = b_i b_{i+\alpha}$ is the nearest-neighbor pair annihilation operator along α direction, with $\alpha = \hat{x}, \hat{y}$ or $\hat{y} - \hat{x}$.

In both the SF phase and supersolid phase, the obtained $S(k)$ and $M_b(k)$ show Bragg peaks at the corners of the hexagonal Brillouin zone, e.g., at $k_1 = (\pm 4\pi/3, 0)$. In particular, at small K , both the peak of the density structure factor $S(k)$ and momentum distribution function $M(k)$ are very sharp (not shown). As shown in Fig.3, at large $V = 6.0$, with the increase of K , $S(k_1)$ decreases continuously, while $M_b(k_1)$ increases at first and then decreases with larger K . Eventually both $S(k_1)$ and $M_b(k_1)$ becomes very weak beyond certain critical value of K . On the other hand, $M_p^\alpha(k)$ shows peaks at zero momentum, i.e., $k_0 = (0, 0)$, and will increase with K , $M_p^\alpha(k)$ increases monotonically before phase separation. One can obtain the corresponding order parameters in the thermodynamic limit based on the finite-size scaling of the

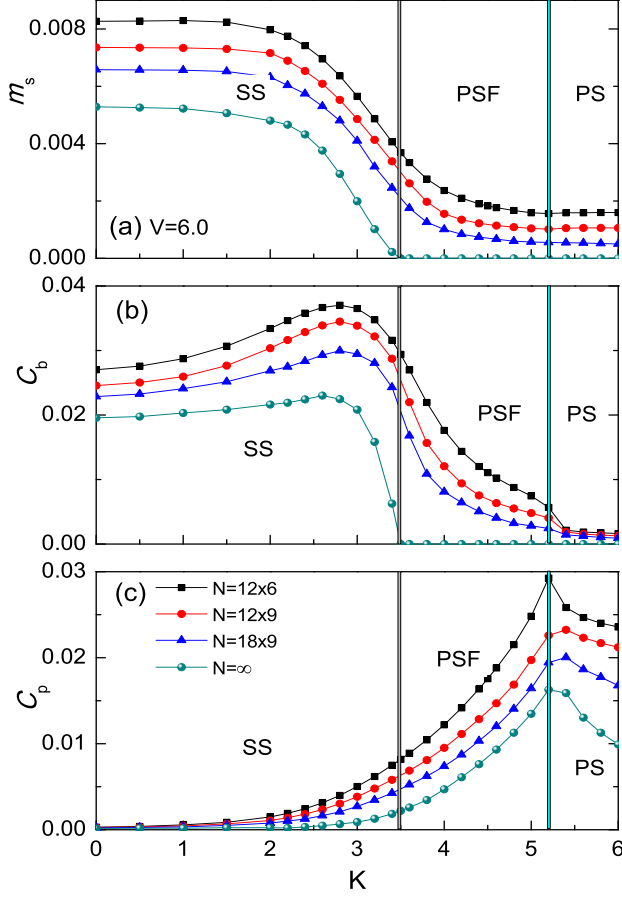


FIG. 3: (color online) (a) The density structure factor order parameter m_s , (b) atomic condensate density C_b at momentum $k_1 = (4\pi/3, 0)$, and (c) pair condensate density C_p at momentum $k_0 = (0, 0)$, as functions of K at $V = 6.0$ and filling $\rho = 1/6$, respectively, with system size $N = 12 \times 6$, 12×9 , 18×9 , and the corresponding extrapolations in the thermodynamic limit.

peak values $S(k_1)$, $M_b(k_1)$ and $M_p^\alpha(k_0)$. Specifically, the structure factor order parameter and the boson condensate density can be determined by $m_s = S(k_1)/N$ and $C_b = M_b(k_1)/N$, while the total pair condensate density is given by $C_p = \sum_\alpha C_p^\alpha = \sum_\alpha M_p^\alpha(k_0)/N$. Examples of these order parameters are shown in Fig.3 as a function of correlated hopping K with $N = 12 \times 6$, 12×9 and 18×9 .

Nonzero m_s and C_b in the thermodynamic limit correspond to the diagonal long-range order (LRO) and off-diagonal long-range order (ODLRO), respectively. Examples of the finite-size scaling are shown in Fig.4 by plotting m_s , C_b and C_p as functions of $1/N$, at $V = 6.0$ and different K , using quasi-2D lattice geometry with system size up to $N = 18 \times 9$. The obtained order parameters extrapolated to the thermodynamic limit are presented in Fig.3 (dark cyan sphere) and Fig.4. It is worth noting that after extrapolation both m_s and C_b continuously decrease to zero simultaneously at the criti-

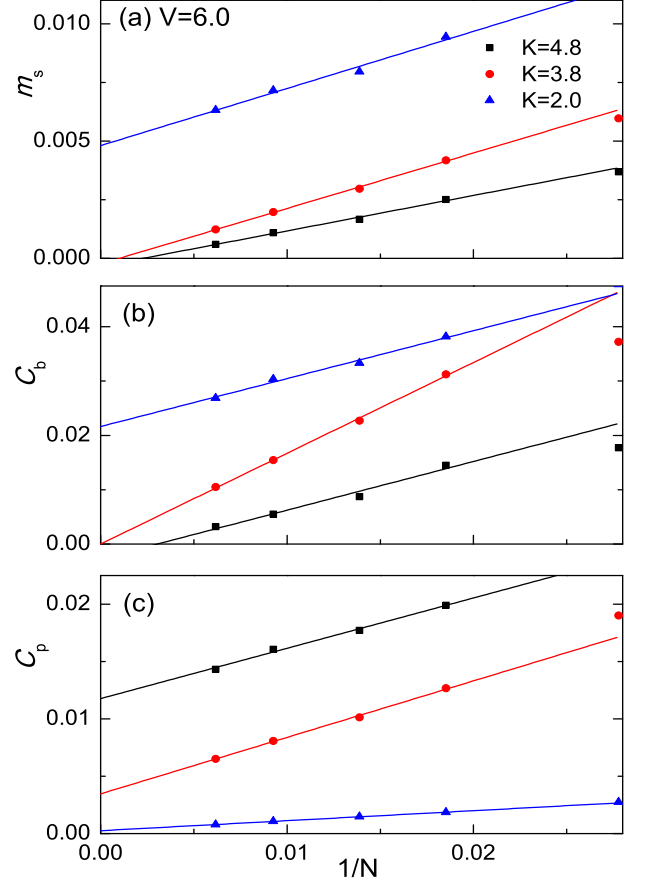


FIG. 4: (color online) Examples of finite-size scaling of (a) the density structure factor order parameter m_s and (b) atomic condensate density C_b at momentum $k_1 = (4\pi/3, 0)$, as well as (c) the pair condensate density C_p at momentum $k_0 = (0, 0)$, for different K at $V = 6.0$ and filling $\rho = 1/6$, with system size up to 18×9 .

cal K , and the system enters the pair superfluid phase in the thermodynamic limit, indicating a continuous phase transition. However, C_p is nonzero in both the SS and PSF, and it always increases monotonically with K (See Fig. 3(c)) before phase separation. Specifically, the finite-size scaling for C_p at $K = 2.0$ in the supersolid phase gives us a small but finite value $C_p \approx 2.5 \times 10^{-4}$ (around 2% of C_p at $K = 4.8$), as shown in Fig.4(c).

With the decrease of the repulsive interaction V , both the supersolid phase and pair superfluid phase become weaker and move to smaller K . In particular, a superfluid phase appears at small K locating at the left bottom corner in the phase diagram (see Fig.2). Compared with the supersolid and pair superfluid phase at large V , the pair condensate density at $k_0 = (0, 0)$ becomes zero, i.e., $C_p(k_0) = 0$. Even with the absence of the repulsive interaction V , the atomic superfluid phase is completely suppressed with the increase of K and give way to the supersolid phase through a first-order transition around

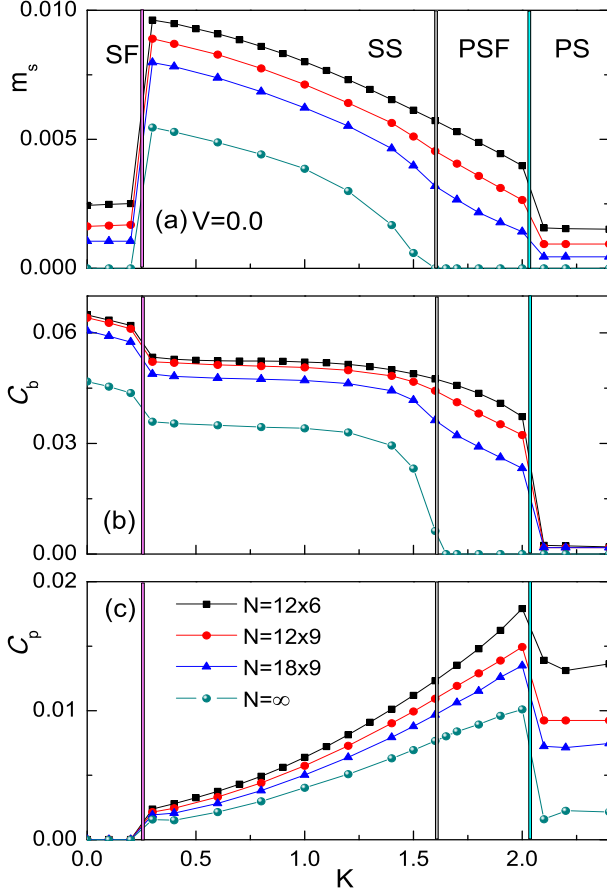


FIG. 5: (color online) (a) The density structure factor order parameter m_s , (b) atomic condensate density C_b at momentum $k_1 = (4\pi/3, 0)$, and (c) the pair condensate density C_p at momentum $k_0 = (0, 0)$, as functions of K at $V = 0.0$ and filling $\rho = 1/6$, respectively, with system size $N = 12 \times 6$, 12×9 and 18×9 , as well as the corresponding extrapolations in the thermodynamic limit.

$K = 0.3$. This can be seen clearly in Fig.5, in which m_s and C_p jump from zero to a finite value in the thermodynamic limit, while C_b encounters a sharp drop to a smaller but still finite value. It is interesting to note that the pair superfluid phase still remains robust in a finite parameter region $K \approx 1.6 - 2.0$, even in the absence of the repulsive interaction V , due to the competition between t and K . Finally, the system becomes phase separated when K becomes dominant.

IV. THEORETICAL UNDERSTANDING

In this section, we develop a simple Landau-Ginzburg theory to describe the supersolid, superfluid and paired superfluid phases on the triangle lattice, including the phase transitions between them. The dispersion of a boson with frustrated hopping in triangular lattice has two

minimums at \vec{K} and $-\vec{K}$, where $\vec{K} = (4\pi/3, 0)$. Therefore we introduce the two $U(1)$ order parameters $\phi_{1,2}$ for boson condensate at $\pm\vec{K}$

$$b^\dagger(\vec{x}) \sim \phi_1(\vec{x})e^{i\vec{K}\cdot\vec{x}} + \phi_2(\vec{x})e^{-i\vec{K}\cdot\vec{x}} \quad (5)$$

Under time reversal and lattice symmetries, $\phi_{1,2}$ transform as follows:

$$\begin{aligned} T_i &: \phi_1 \rightarrow \phi_1 e^{-i2\pi/3}, \phi_2 \rightarrow \phi_2 e^{i2\pi/3}, \quad i = 1, 2, 3 \\ C_6 &: \phi_1 \rightarrow \phi_2, \phi_2 \rightarrow \phi_1 \\ M_x &: \phi_1 \rightarrow \phi_2, \phi_2 \rightarrow \phi_1 \\ \Theta &: \phi_1 \rightarrow \phi_2, \phi_2 \rightarrow \phi_1 \\ U(1) &: \phi_1 \rightarrow \phi_1 e^{i\theta}, \phi_2 \rightarrow \phi_2 e^{i\theta}, \end{aligned} \quad (6)$$

Here T_i are translations by the three unit vector \mathbf{a}_i of the triangle lattice: $\mathbf{a}_1 = (1, 0)$, $\mathbf{a}_2 = (-1/2, \sqrt{3}/2)$, $\mathbf{a}_3 = (-1/2, -\sqrt{3}/2)$. C_6 is $\pi/3$ rotation. M_x is reflection about x axis. Θ is time-reversal transformation. $U(1)$ is the global phase transformation.

The supersolid phase is characterized by *two* nonzero condensate order parameters ϕ_1 and ϕ_2 , which have momentum \vec{K} and $-\vec{K}$ respectively. The coexistence of these two superfluid order necessarily induces a nonzero density wave order $\rho \sim \phi_1^* \phi_2$ at momentum $2\vec{K} = -\vec{K}$, where we have used the fact $3\vec{K} = 0$ up to a reciprocal lattice vector in triangular lattice. The presence of both superfluid and density-wave order taken together signals a supersolid phase, as we found numerically. On the other hand, the paired superfluid phase is characterized by a nonzero pair condensate order parameter Δ at zero momentum, whereas both ϕ_1 and ϕ_2 are disordered.

Since the supersolid phase has a lower symmetry than the paired superfluid phase, the phase transition can be understood as the development of long-range single boson superfluid in the paired superfluid (disordered) phase within the framework of Landau-Ginzburg theory in 2+1 dimension. The effective Landau-Ginzburg Lagrangian, whose form is dictated by the symmetry property (6), is given by

$$\begin{aligned} \mathcal{L} = & \frac{r}{2}(\phi_1^* \phi_1 + \phi_2^* \phi_2) - (\Delta \phi_1^* \phi_2^* + \Delta^* \phi_1 \phi_2) \\ & + u(|\phi_1|^4 + |\phi_2|^4) + 2u_{12}|\phi_1|^2|\phi_2|^2 + v(\phi_1^{*3}\phi_2^3 + \phi_1^3\phi_2^{*3}) \end{aligned}$$

As r decreases, ϕ_1 and ϕ_2 become nonzero, which signals the onset of superfluid order as well as the associated density wave order $\phi_1^* \phi_2$. Note that the pair order parameter Δ is nonzero across the transition. Without loss of generality, Δ is chosen to be real and positive. Due to the trilinear coupling term between Δ , ϕ_1 and ϕ_2 , \mathcal{L} is minimized by $\phi_2^* = \phi_1 \equiv \phi$, where ϕ is *complex*. The last term in S is symmetry allowed for the triangular lattice, and locks the relative phase between ϕ_1 and ϕ_2 , and pins the phase of $\rho = \phi_1 \phi_2^* = \phi^2$ to three distinct values corresponding to three degenerate density wave patterns in the supersolid phase. In terms of ϕ , \mathcal{L} is given by

$$\mathcal{L} = |\partial_\mu \phi|^2 + r_1 |\phi|^2 + u' |\phi|^4 + v(\phi^6 + \phi^{*6}). \quad (7)$$

Except for the last term, \mathcal{L} is the standard complex scalar field theory in 2+1 dimension, and this transition belongs to the 3d XY universality class with order parameter ϕ . By power-counting, the sixth-order phase-locking term is strongly irrelevant at the critical point, thus this transition is continuous.

Interestingly, the above XY transition differs from conventional paired to single boson superfluid transition, which lies in the Ising universality class. The distinction arises from the fact that the superfluid phase studied here has two coexisting (rather than one) condensate order parameters, of which the relative phase is a well-defined physical quantity associated with the density wave order. Our theory can be directly tested by further numerical studies on the critical exponent for the physical order parameter at the quantum critical point. For example, the critical exponent ν take the value of the ordinary 3d XY transition: $\nu \sim 0.67$. Also, the density wave order parameter $\rho \sim \phi^2$ is a bilinear of ϕ in Eq. 7, thus our theory predicts that the order parameter ρ has an anomalous dimension $\eta \sim 1.49$. These predictions can be verified by further numerical studies on model Eq. 1.

We can also interpret the supersolid to pair superfluid transition in terms of the topological defects inside the supersolid phase. For convenience, let us rewrite the fields ϕ_1 and ϕ_2 introduced in Eq. 5 as follows:

$$\phi_1 = \phi \psi, \quad \phi_2 = \phi^* \psi. \quad (8)$$

ϕ and ϕ^* are complex fields that carry lattice momentum \vec{K} and $-\vec{K}$ respectively, while ψ carries the U(1) symmetry of the original boson operator b_i . Thus the boson density wave order parameter is $\rho \sim \phi_1 \phi_2^* \sim \phi^2$, and the pair superfluid order parameter is $b_i b_{i+\alpha} \sim \phi_1 \phi_2 \sim \psi^2$.

In Eq. 8, because ϕ_1 and ϕ_2 are both physical degrees of freedom, ϕ and ψ are defined up to a Z_2 gauge ambiguity, *i.e.* the physics is unchanged under transformation $\phi \rightarrow -\phi$, $\psi \rightarrow -\psi$. The supersolid phase corresponds to the case where both ϕ and ψ are condensed, while in the pair superfluid phase only ψ is condensed. Inside the supersolid phase, the smallest superfluid vortex, has only π -vorticity, *i.e.* it is a bound state between a π -vortex of ψ and a π -vortex of ϕ . In other words, both ψ and ϕ will change sign after encircling this vortex, while the physical degree of freedom is unchanged. Notice that the π -vortex of ϕ is a full vortex of boson density wave order ρ , which is equivalent to a *dislocation* of the density wave pattern.

Starting with the supersolid phase, if we want to drive a transition into the pair superfluid phase, we need to

“melt” the boson density wave order by condensing its defects. However, since the pair superfluid phase also has a half quantum π -vortex, this transition cannot be driven by condensing the smallest π -vortex discussed in the previous paragraph. Instead, it must be driven by the condensation of the 2π -vortex of ϕ , which only melts the boson density wave, but leaves the superfluid stiffness unaffected. Since the physical boson density wave order parameter $\rho \sim \phi^2$ is a bilinear of ϕ , this transition is driven by condensing a “double” dislocation of ρ . Thus this transition is analogous to the transition between pair-density-wave and charge-4e superconductor discussed in Ref.¹³.

V. SUMMARY AND EXTENSION

We have studied a hard-core Bose-Hubbard model with an unusual correlated hopping on a triangular lattice using density-matrix renormalization group method. In the phase diagram, we discovered a supersolid phase and a pair superfluid phase, in addition to the standard superfluid phase. The supersolid and pair superfluid phases were discussed separately before in different spin models^{17–19,22}. However, to our knowledge it is the first time that both these phases are realized in one model. We also theoretically establish that the phase transition between the supersolid phase and the pair superfluid phase is continuous.

If the phase coherence and superfluid stiffness of the pair superfluid phase are destroyed, then the system most likely enters a fully gapped Z_2 liquid phase with the same topological order as the toric code model²¹. Presumably this new transition can be obtained by turning on some extra terms in the Hamiltonian. We will leave this to future study.

VI. ACKNOWLEDGEMENT

We would like to thank Matthew Fisher, Steve Kivelson, W. Vincent Liu, Senthil Todadri, and especially Leon Balents and Fa Wang for insightful discussions. This work was partially supported by the KITP NSF grant PHY05-51164 and the NSF MRSEC Program under Award No. DMR 1121053, and the NBRPC (973 Program) 2011CBA00300 (2011CBA00302). Cenke Xu is supported by the Sloan Foundation. Liang Fu is supported by start-up funds of MIT.

¹ M. P. A. Fisher, P. B. Weichman, G. Grinstein, and D. S. Fisher, *Phys. Rev. B* **40**, 546 (1989).

² L. Balents, M. P. A. Fisher, and S. M. Girvin, *Phys. Rev. B* **65**, 224412 (2002).

³ S. V. Isakov, Yong Baek Kim, A. Paramekanti, *Phys. Rev.*

Lett. **97**, 207204 (2006).

⁴ S. V. Isakov, M. B. Hastings, R. G. Melko, *Nature Physics* **7**, 772 (2011).

⁵ T. Senthil and O. Motrunich, *Phys. Rev. B* **66**, 205104 (2002).

- ⁶ S. V. Isakov, R. G. Melko, M. B. Hastings, *Science* **335**, 193 (2012).
- ⁷ M. S. Block, R. V. Mishmash, R. K. Kaul, D. N. Sheng, O. I. Motrunich, M. P. A. Fisher, *Phys. Rev. Lett.* **106**, 046402 (2011).
- ⁸ M. S. Block, D. N. Sheng, O. I. Motrunich, M. P. A. Fisher *Phys. Rev. Lett.* **106**, 157202 (2011).
- ⁹ R. V. Mishmash, M. S. Block, R. K. Kaul, D. N. Sheng, O. I. Motrunich, M. P. A. Fisher *Phys. Rev. B* **84**, 245127 (2011).
- ¹⁰ H. C. Jiang, Z. Y. Weng, D. N. Sheng, *Phys. Rev. Lett.* **101**, 117203 (2008).
- ¹¹ S. Yan, D. A. Huse, S. R. White, *Science* **332**, 1173 (2011).
- ¹² H. C. Jiang, H. Yao, L. Balents, arXiv:1112.2241, (2011).
- ¹³ E. Berg, E. Fradkin, S. A. Kivelson *Nature Physics* **5**, 830 (2009).
- ¹⁴ E. G. Moon, *arXiv:1202.5389*.
- ¹⁵ S. R. White, *Phys. Rev. Lett.* **69**, 2863 (1992); **77**, 3633 (1996).
- ¹⁶ E. M. Stoudenmire and S. R. White, arXiv:1105.1374.
- ¹⁷ R. G. Melko, A. Paramekanti, A. A. Burkov, A. Vishwanath, D. N. Sheng, L. Balents, *Phys. Rev. Lett.* **95**, 127207 (2005).
- ¹⁸ H. C. Jiang, M. Q. Weng, Z. Y. Weng, D. N. Sheng and L. Balents, *Phys. Rev. B*, **79**, 020409(R) (2009).
- ¹⁹ F. Wang, F. Pollmann, and A. Vishwanath, *Phys. Rev. Lett.* **102**, 017203 (2009).
- ²⁰ H. C. Jiang et al. (Unpublished).
- ²¹ A. Yu. Kitaev, *Ann. Phys. (N.Y.)* **303**, 2 (2003).
- ²² Lars Bonnes, Stefan Wessel, *Phys. Rev. Lett.* **106**, 185302 (2011).